Focus and Shoot: Exploring Auto-Focus in RFID Tag Identification Towards a Specified Area

Yafeng Yin, *Student Member, IEEE*, Lei Xie, *Member, IEEE*, Jie Wu, *Fellow, IEEE*, and Sanglu Lu, *Member, IEEE*

Abstract—With the rapid proliferation of RFID technologies, RFID has been introduced into applications such as inventory and sampling inspection. Conventionally, in RFID systems, the reader usually identifies all the RFID tags in the interrogation region with the maximum power. However, some applications may only need to identify the tags in a specified area, which is usually smaller than the reader's default interrogation region. An example could be identifying the tags in a box, while ignoring the tags out of the box. In this paper, we respectively present two solutions to identify the tags in the specified area. The principle of the solutions can be compared to the picture-taking process of an auto-focus camera, which firstly focuses on the target automatically and then takes the picture. Similarly, our solutions first focus on the specified area and then shoot the tags. The design of the two solutions is based on the extensive empirical study on RFID tags. Realistic experiment results show that our solutions can reduce the execution time by 44 percent compared to the baseline solution, which identifies the tags with maximum power. Furthermore, we improve the proposed solutions to make them work well in more complex environments.

Index Terms—RFID, tag identification, auto-focus, specified area, experimental study, algorithm design

✦

1 INTRODUCTION

RECENTLY, RFID tags have been widely used in various applications, such as inventory control, sampling inspection, and supply chain management. Each RFID tag has a unique ID, thus the reader can recognize the object by identifying its attached tag. Many existing research works on RFID have concentrated on tag identification [1], [2], [3], [4], [5], [6], [7], [8], aiming to identify a large number of tags as quickly as possible. While detecting the missing tags and searching a particular subset of tags only concentrate on the part of tags. However, all the literature do not research the problem of tag identification in a specified area, which is rather important in many applications, e.g., inventory and sampling inspection in warehouse management. Taking the inventory for example, in order to have a knowledge of the tags in the target area, we may only need to identify the tags in some specified boxes while ignoring the others, i.e., identifying the tags in the specified area. In regard to a sampling inspection, it also requires focusing on the tags in the current area, while ignoring the others. Sometimes, it is difficult to move the objects out for tag identification, especially for the objects obstructed by obstacles. A traditional solution is to identify the tags with the maximum power (MaxPw). However, this solution will identify the tags out of the area, leading to lower accuracy of the identification process.

Moreover, identifying the tags out of the area is rather time-consuming. Due to the large number of tags, time-efficiency is very important. Therefore, it is essential to identify the tags in the specified area efficiently without moving the tags.

Fortunately, we note that tag identification in the specified area can be compared to the picture-taking process in an auto-focus camera. The camera automatically focuses on the object before shooting, aiming to lock the target object while ignoring the others. In this paper, we propose the photography based identification method, which works in a similar way. It first focuses on the specified area by adjusting the antenna's angle and the reader's power, and then identifies the tags in the area. When the reader's interrogation region is just enough to cover the specified area, it achieves the best performance. To solve this problem, we respectively propose two solutions working in the realistic environments. Both solutions conform to the EPC-C1G2 standards.

However, efficiently identifying the tags in realistic environments is difficult. There are a few research works concentrating on this problem. The reading performance in the realistic experiments is still unknown, especially for a large number of tags. Hence, we conduct a series of measurements over RFID tags in realistic settings, investing the factors which affect the reading performance. Fortunately, we have a few important new findings. For example, we find that the tag density affects the effective scanning range, i.e., the larger the tag density, the smaller the effective scanning range. The findings are crucial for improving the performance of our solutions. They indicate that the reader should adaptively adjust its interrogation region, considering the actual situation. We propose the two solutions based on the extensive experimental study, in order to make the solutions work well in the realistic environments.

- *Y. Yin, L. Xie, and S. Lu are with the State Key Laboratory for Novel Software Technology, Nanjing University, Nanjing 210023, China. E-mail: yyf@dislab.nju.edu.cn, {lxie, sanglu}@nju.edu.cn.*
- *J. Wu is with the Department of Computer and Information Sciences, Temple University, Philadelphia, PA 19122. E-mail: jiewu@temple.edu.*

We make the following contributions in this paper.

- We conducted extensive experiments on the commodity RFID system in the realistic environments, and investigated the factors affecting the reading performance.
- To the best of our knowledge, this is the first work investigating efficient tag identification in the specified area, which is essential for many applications, such as inventory and sampling inspection. We propose the photography-based identification method, which works in a way similar to a camera. Besides, we respectively propose two solutions to solve the problem, and reduce the execution time by 44 percent compared to the baseline solution. Moreover, we improve the proposed solutions to make them work well in the more complex environments.
- Our solutions work in the realistic environments with the commercial RFID system, which do not require any changes to the protocols and the low-level parameters in the system. Both of the two solutions conform to the EPC-C1G2 standards.

2 RELATED WORK

Previous research on RFID concentrates on designing anti-collision ID-collection protocols to collect all the tag IDs. The existing anti-collision protocols can be categorized as being either tree-based [1], [2], [3], [4] or ALOHA-based [5], [6], [7], [8]. Tree-based protocols resolve collisions by muting subsets of tags that are involved in a collision. ALOHA-based protocols assign a distinct transmission time slot to each tag, and sequentially identify the tags.

Instead of identifying all the RFID tags, protocols for identifying missing tags monitor a set of tags and detect the missing-tag event [9], [10], [11], [12], [13], [14]. Unknown tag identification aims to identify the tags (e.g., the new added tags or the misplaced tags), which appear to be unknown by the reader(s) currently covering them [15], [16]. Unknown-target information collection needs to find out the target tags and read the information from them [17]. Fast tag searching aims to quickly search the particular tag IDs [18]. Besides, the polling-based protocols are proposed to collect the information from RFID tags in a time/energy-efficient approach [19], [20]. Rather than identifying the tags, the RFID cardinality estimation protocols count the number of distinct tags [21], [22], [23], [24], which can serve as useful inputs to improve the efficiency of tag identification [25], [26].

The above research works mainly consider the situation without considering issues like path loss, energy absorption, multipath effect, etc. While considering the impact of the physical layer's unreliability, Buettner and Wetherall [27] examine the performance of the C1G2 RFID system in a realistic setting. Aroor and Deavours [28] use a simple, empirical, experimental approach to identify the state of the technical capability of passive UHF RFID systems. Xie et al. [29] conduct an extensive experimental study on the mobile RFID system, and build a model to depict how various parameters affect the reading performance.

Different from the related work, our research focuses on identifying the tags in the specified area while ignoring the tags outside the area. Besides, our solutions work in the
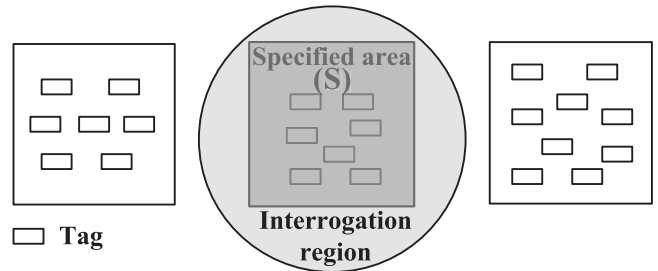

Fig. 1. Identify the tags in the specified area.

realistic environment. We aim to identify as many tags in the specified area as possible, while minimizing the execution time.

3 PROBLEM FORMULATION

3.1 System Model

Each object is attached with an RFID tag, which has a unique ID. In this paper, we use the terms 'object' and 'tag' interchangeably. The number of tags and the distribution of tag IDs are unknown. The reader is statically deployed and configured with an antenna. The antenna is associated with an interrogation region, within which the reader can identify the tags. The antenna is deployed in a fixed position, e.g., it can be fixed on the wall or the ceiling. It cannot change its distance to the objects, but it can be rotated, just like the electric fan fixed on the ceiling. This can be a typical setting for the application scenarios like inventory and sampling inspection in warehouse management. By rotating the antenna, we can identify more tags with fewer readers. Besides, the reader can control the interrogation region by adjusting the power.

The objects are packaged in boxes. The boxes out of the specified area S have reasonable distances between the boxes in S, which means that the area S has a clear boundary. As shown in Fig. 1, the tags in S are called *target tags*, while the tags outside S are called *interference tags*. The objective of this paper is to identify as many *target tags* as possible, while minimizing the execution time.

3.2 Performance Metrics

We consider the three performance metrics for evaluating the solution's efficiency.

1) *Coverage ratio ρ constraint*. Let S be the set of tags in S (target tags), $s = |S|$. Let M be the set of the tags that are identified in S, $m = |M|$. Obviously, $M \subseteq S$ and $m \leq s$. Then, $\rho = \frac{m}{s}$, $0 \leq \rho \leq 1$. The larger the value of ρ, the better the coverage ratio. Given a constant α, ρ should satisfy $\rho \geq \alpha$. α is related to the specific scenario: when the environment and the deployment of the RFID system are fixed, the value of α can be determined.

2) *Execution time T*. It represents the duration of the whole process. It shows the time efficiency, which is rather important, especially for the identification of a large number of tags. The smaller the time T, the better the time efficiency.

3) *Misreading ratio λ*. Let U be the set of tags out of S (interference tags) that are identified, $u = |U|$, $U \cap S = \emptyset$. Then, $\lambda = \frac{u}{u+m}$. The smaller the value of λ, the lower the misreading ratio.

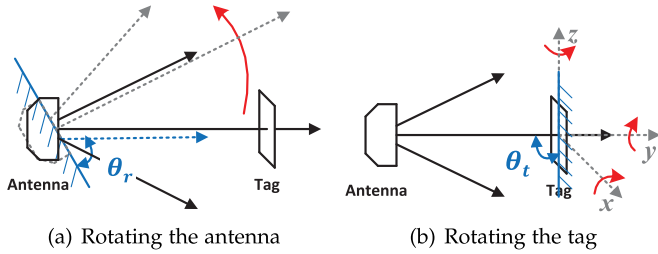(a) Rotating the antenna   (b) Rotating the tag

Fig. 2. Identify the tag at different angles.

The objective of this paper is to minimize the execution time T, while the coverage ratio satisfies $\rho \geq \alpha$. When $\rho \geq \alpha$, minimizing T means avoiding identifying the *interference tags*, in order to reduce the identification time. There is no constraint on λ, which is related to T. However, for the same execution time, the lower the misreading ratio, the better the performance of a solution.

4   OBSERVATIONS FROM THE REALISTIC EXPERIMENTS

In order to know the factors affecting the reading performance in real environments, we conduct the following experiments. We use the Alien-9900+ reader and Alien-9611 antenna. The reader's maximal power $\max P_w$ is 30.7 dBm and its minimal power $\min P_w$ is 15.7 dBm. The RFID tag is

the Alien-9640 tag. Each tag is attached into a distinct book. The antenna and the books are placed on the tablet chairs with a height of 0.5 m. Unless otherwise specified, we make the antenna face towards the center of the objects, set the reader's power $P_w = 30.7$ dBm, and the distance between the tags and the antenna $d = 1$m. For each experiment, the reader scans the tags for 50 cycles.

4.1   Identifying the Tag at Different Angles

As the angle between the radiation direction and the surface of the antenna deceases, the reading performance usually deceases. Besides, the placement of the tag may affect the reading performance. As shown in Fig. 2, we respectively rotate the antenna and the tag to observe the minimal power $P_{w_{min}}$ needed to activate one tag. Firstly, we rotate the antenna while keeping the tag unchanged. We use θ_r (see Fig. 2a) to represent the angle between the antenna's radiation direction and the antenna's surface, $\theta_r \in [0°, 90°]$. Fig. 3a shows that as θ_r decreases, $P_{w_{min}}$ becomes larger. When the antenna faces towards the tag ($\theta_r = 90°$), it achieves the best reading performance. Secondly, we rotate the tag while keeping the antenna unchanged. We use θ_t (see Fig. 2b) to represent the angle between the radiation direction and the tag's surface. We respectively rotate the tag along the x-axis, y-axis, and z-axis, as shown in Fig. 2b. Fig. 3a shows when the tag rotates along the x-axis, θ_t decreases, $P_{w_{min}}$ becomes

(a) Minimal power vs. angles (Group 1)

(b) Distribution of identified tags vs. powers

(c) Identified tag IDs vs. powers

(d) Coverage ratio vs. distances

(e) Scanning range vs. tag densities

(f) Number of identified tags vs. tag cardinality

(g) Identification ratio vs. materials

(h) Minimal power vs. angles (Group 2)

(i) Minimal power vs. angles (Group 3)

(j) Minimal power vs. angles (Group 4)

(k) Minimal power vs. angles (Group 5)

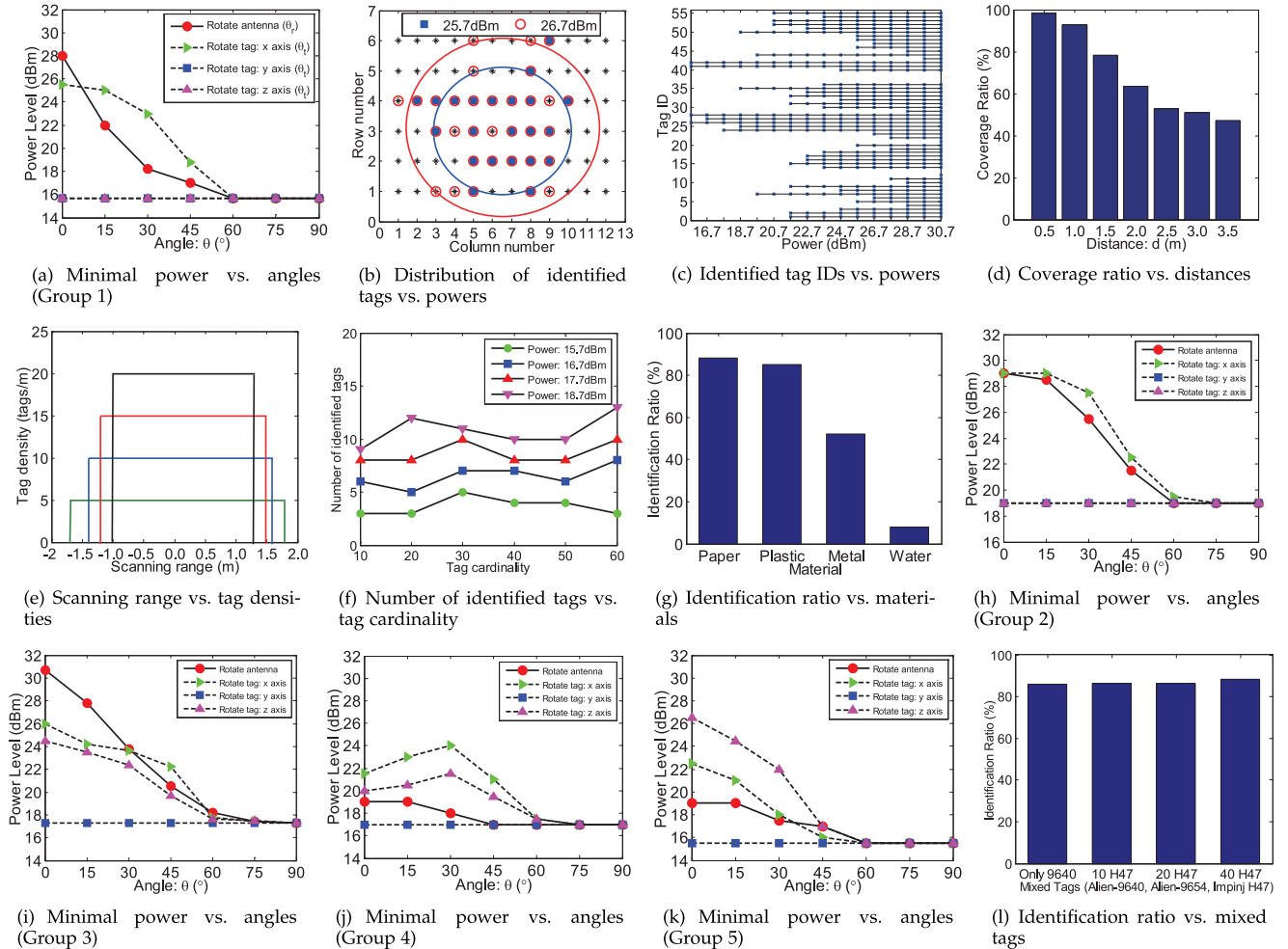(l) Identification ratio vs. mixed tags

Fig. 3. Observations from the realistic experiments.

TABLE 1
Combinations of Different Readers, Antennas, and Tags

	Reader	Antenna (Polarization mode)	Tag (IC type; Antenna technology)
1	Alien-9900+	Alien-9611 (Circular)	Alien-9640 (Alien Higgs-3; Dipole)
2	Alien-9650	Alien-9650 (Circular)	Alien-9654 (Alien Higgs-3; Dipole)
3	Alien-9900+	Alien-9611 (Circular)	Impinj H47 (Monza 4; Dual-differential)
4	Impinj R420	Impinj Threshold (Linear)	Impinj H47 (Monza 4; Dual-differential)
5	Impinj R420	Impinj Threshold (Linear)	Alien-9640 (Alien Higgs-3; Dipole)

larger. When the tag rotates along the y-axis, θ_t keeps unchanged, thus $P_{w_{min}}$ keeps unchanged. When the tag rotates along the z-axis, although θ_t decreases, the tag is easily identified. Even though the tag holds the same angle θ_t, the different placement of the tag may result in different reading performances.

It is best to identify the tags with $\theta_r = 90°$ and $\theta_t = 90°$. However, we may have no access to the placement of each tag, then we should try to make the antenna face towards the tags ($\theta_r = 90°$) to improve the reading performance.

4.2 Adjusting the Reader's Power

The larger the reader's power, the larger the interrogation region, but the new identified tags may not be located in the interrogation region's boundary. However, if a tag can be identified with a low power, it must be identified with a larger power. We uniformly deploy 72 tags on the wall. The distance between two adjacent tags is 20 cm, as shown in Fig. 3b. The new identified tags may not be in the interrogation region's boundary. We cannot distinguish a tag's position by only adjusting the power. However, Fig. 3c shows that if a tag can be identified with a low power, then it definitely can be identified by a larger power. Usually, the large power can increase the number of identified tags.

4.3 Varying the Distance between the Tags and the Antenna

As the distance between the tags and the antenna increases, the reading performance decreases. Besides, when the distance is fixed, the maximum coverage ratio has an upper bound, whatever the reader's power is. We vary the distance d from 0.5 to 3.5 m. Fig. 3d shows that as d increases, the identified tag cardinality decreases. When d is small (e.g., $d \leq 1.5$ m), the reading performance is relatively good. However, when the distance and the number of tags are fixed, the coverage ratio has an upper bound. For example, when $d = 1.5$ m and $n = 55$, the maximum coverage ratio is 78 percent. Fortunately, some applications (e.g., sampling inspection) just need the coverage ratio to meet the constraint instead of achieving 100 percent. However, when considering the high coverage ratio, the antenna should not be placed far away from the tags.

4.4 Effect of the Tag Cardinality

The tag cardinality can affect the effective interrogation region. However, it has a little effect on the number of identified tags. We uniformly deploy the tags in a row with length 4 m and vary the number of tags (tag cardinality) as 20, 40, 60, 80. As shown in Fig. 3e, given a fixed power (30.7 dBm), as the tag cardinality increases, the effective interrogation region decreases. Therefore, when the tag cardinality in

the specified area (tag density) is unknown, we can not calculate the interrogation region accurately. However, if we only want to identify a few tags (e.g., for sampling), we can choose an estimated power, because the tag cardinality has a little effect on the number of identified tags, as shown in Fig. 3f.

4.5 Effect of the Materials of Objects

The materials of the objects can affect the reading performance, especially for metal materials and water-containing materials. We respectively attach 60 tags to the books, plastic clips, iron clips, and milk. The corresponding materials of the objects are paper, plastic, metal, and water. Fig. 3g shows the materials can greatly affect the reading performance. The reading performance for the tags attached to the metal materials is not good, due to the reflection of the metal materials. The reading performance for the tags attached to the water-containing materials is poor, due to the energy absorbtion in the water. In this case, we can use the functional tags tailored to specific materials (such as anti-metal tags against metal) to tackle this issue.

4.6 Different Types of Tags and Antennas

The types of the tags and the antennas can affect the reading performance. However, the tags and the antennas belonging to the same series may have the similar reading performance. As shown in Table 1, we use five different groups of RFID systems to repeat the experiments in Section 4.1. The experiment result in group 1 is shown in Fig. 3a. While the experiment results in group 2, 3, 4, 5 are shown in Figs. 3h, 3i, 3j, and 3k, respectively. By comparing Fig. 3a and Figs. 3i, 3j, and 3k, we can find that different types of antennas and tags will result in different reading performances. This is mainly caused by the polarization mode of the antenna, the IC type and the antenna technology of the tag, and the matching way between the antenna and the tag. While comparing Figs. 3a and 3h, we can find that the two RFID systems have the similar reading performance, because the components in group 1 and group 2 belong to the same series.

In addition to this, we conduct another experiment by mixing different types of tags. The 60 tags are consisted of Aline-9640 tags, Alien-9650 tags and Impinj H47 tags. Becuase Alien-9640 tags and Alien-9654 tags have the similar performance, we vary the number of Impinj H47 tags to observe the reading performance. Impinj H47 is the omni-directional tag, which is insensitive to the placement of tag. When the proportion of H47 increases, the reading performance becomes better, as shown in Fig. 3l. However, the combinations of different types of tags have a little effect on
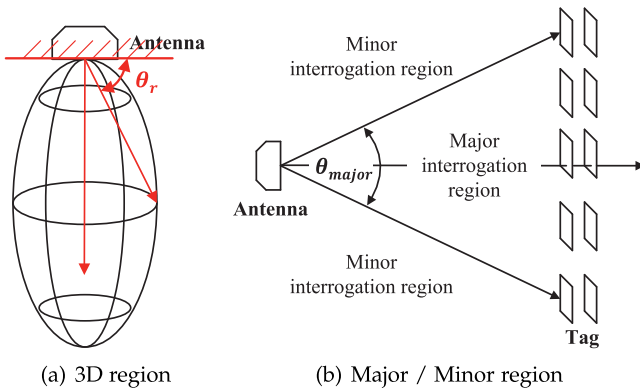
(a) 3D region   (b) Major / Minor region

Fig. 4. The model of an antenna's interrogation region.

Fig. 5. The framework of PID.

the reading performance. When the tags are located in the center area of the interrogation region, the tags usually can be identified easily.

4.7 Analysis

Based on the above observations, we can use the model shown in Fig. 4 to describe the interrogation region of an antenna. In the three-dimensional space, the interrogation region is like an ellipsoid, as shown in Fig. 4a. We further divide the interrogation region into *major interrogation region* and *minor interrogation region*, as shown in Fig. 4b. In the *major interrogation region*, the reader usually has good reading performance. While in the *minor interrogation region*, the reading performance is usually poor. Based on Fig. 3, the range of major interrogation region for Alien-9611 antenna is about $\theta_{major} = 60°$, which is almost consistent to the 3 dB beamwidth (65 degree) of Alien-9611 antenna.

However, Fig. 3 illustrates that the radiation angle θ_r, the placement of the tag, reader's power P_w, the distance d between the tags and the antenna, the tag density, the tag cardinality, the material the tag is attached to, and the types of antennas and tags all affect the reading performance. Therefore, we use the above model as a guide. We will not depend on the model to calculate the parameters in our algorithms. Fortunately, when the tags are located in the major interrogation region, they usually can be identified easily. As a result, instead of concentrating on the influence from tags, we concentrate on adjusting the antenna's radiation angle θ_r and the reader's power P_w to focus on the specified area. Unless otherwise specified, we use Alien-9900+ reader, Alien-9611 antenna, and Aline-9640 tag in this paper.

According to the above analysis, we conclude the following clues to design our solutions.

- *Rotating the antenna*. If the objects are placed with a reasonable distance, we can distinguish them by rotating the antenna, based on the different reading performances in major/minor interrogation regions.
- *Facing towards the target tags*. Due to the good performance in major interrogation region, we rotate the antenna to face towards the target tags.
- *Power stepping*. We can adjust the power to make the interrogation region be just cover the specified area,
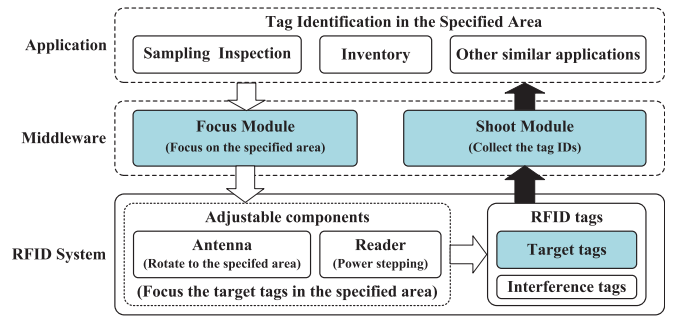
in order to reduce the probability of identifying the interference tags.

5   BASELINE SOLUTIONS

In order to identify the *target tags* in the specified area S, while ignoring the *interference tags*, we should focus on S and identify as many *target tags* as possible. As mentioned in 4.2, the larger the reader's power, the larger the interrogation region. If we only want to focus on the area S, we should use a lower power. On the contrary, if we want to identify more tags, we should use a larger power. Therefore, scanning with the minimal power $\min P_w$ and the maximal power $\max P_w$ are two baseline solutions, which are respectively called as MinPw and MaxPw.

However, if the reader's power is too small, the interrogation region cannot cover the specified area, leading to the low coverage ratio. If the reader's power is too large, the interrogation region may be too large, leading to the identification of the *interference tags*. It increases the time cost and the misreading ratio. Therefore, it is important to use a reasonable power to identify the tags in the specified area.

6   PHOTOGRAPHY BASED IDENTIFICATION WITH DISTANCE MEASUREMENT

In this section, we propose a solution called Photography based tag Identification with Distance measurement (PID), which works with a 3D camera (e.g., a Kinect). The process of PID can be compared to the picture-taking process in a camera. It focuses on the area and shoots the objects, as shown in Fig. 5. The application appoints the specified area S and the middleware collects the tag IDs in S by the RFID systems. It consists of the focus module and the shoot module. The focus module adjusts the reader's power and rotates the antenna to make the interrogation region focus on S. The shoot module collects tag IDs. The two corresponding processes are respectively called *Focusing Process* and *Shooting Process*.

6.1   Focusing Process

The focusing process aims to make the interrogation region focus on the specified area S by adjusting θ_r, P_w, while ignoring the tags outside S. It contains three phases, selecting the initial power, establishing the boundary, and power stepping. The objective of this process is to get the optimal power P_w^*, whose corresponding interrogation region is just enough to cover the specified area S.
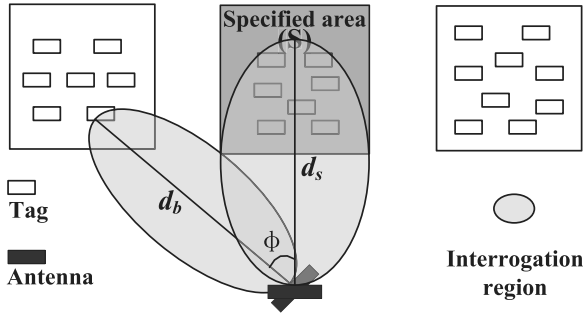
Fig. 6. Identify the tags in S with a 3D camera.

6.1.1 Selecting the Initial Power

Before the reader identifies the tags, it selects the initial power instead of the default (maximum) one to control the interrogation region. In RFID systems, the reader's interrogation region of an antenna is like an ellipsoid. The larger the angle θ_r between the radiation direction and the antenna's surface, the longer the reader's scanning range. However, in the realistic environment, the tag size, the reader's power P_w, the radiation angle θ_r, and the distance d all affect the effective interrogation region, as mentioned in Section 4. Therefore, in the realistic environments, we measure the minimum power (MinPw) $P_{w_{min}}$ based on θ_r and d, and use them to calculate the initial power. In this paper, we measure $P_{w_{min}}(\theta_r, d)$ with the distances $d_j = 0.5\,\text{m} \times j, j \in [1,7]$ and the angles $\theta_i = 90° - 15° \times i, i \in [0,6]$. For example, we get $P_{w_{min}}(90°, 1.0) = 15.7\,\text{dBm}$, $P_{w_{min}}(75°, 1.5) = 18.8\,\text{dBm}$, $P_{w_{min}}(60°, 2.0) = 23.4\,\text{dBm}$. The reader first selects the reference angle θ_i closest to θ_r, $|\theta_r - \theta_i| \leq |\theta_r - \theta_k|$ ($k \in [0,6]$ and $k \neq i$). Then, it uses d to calculate the initial power $P_{w_{min}}(\theta_r, d)$

$$\begin{cases} P_{w_{min}}(\theta_i, d_j) & \text{if } d = d_j \\ \frac{P_{w_{min}}(\theta_i, d_j) + P_{w_{min}}(\theta_i, d_{j+1})}{2} & \text{if } d \in [d_j, d_{j+1}]. \end{cases} \quad (1)$$

However, the power is only used as the initial power. In order to identify more tags, the reader can repeatedly increase the power by ΔP_w. We set $\Delta P_w = 1\,\text{dBm}$, which is achievable by most of the commercial readers [30].

6.1.2 Establishing the Boundary

The 3D camera can recognize the specified area by RGB camera and measure distance by 3D depth sensors. However, the reader can hardly find the boundary of S, due to the unknown distribution of tag IDs. Therefore, PID first establishes the boundary S_b of the area S based on the *interference tags* located around S, as shown in Fig. 6. PID uses the 3D camera to calculate the minimum distance d_b between the *interference tags* in S_b and the antenna, and the distance d_s between the center of S and the antenna. Furthermore, it calculates the rotation angle φ as follows:

$$\varphi = arccos\left(\frac{d_s}{d_b}\right), \varphi \in (0°, 90°). \quad (2)$$

Then, the antenna rotates φ degree to face the *interference tags* in S_b for identification. The identified tags are used as reference tags to describe S_b.

In PID, the antenna always faces towards the center of the objects, $\theta_r = 90°$. Then, the reader selects the initial power

P_{wb} according to the distance d, $P_{wb} = P_{w_{min}}(90°, d)$. If the power P_{wb} is not large enough, the reader increases the power by ΔP_w and identifies n_b tags, as shown in Algorithm 1. It repeats the above process until $n_b \geq n_\varepsilon$, which means that it has collected enough tag IDs $N_b = \{ID_1, ID_2, \ldots, ID_{n_b}\}$ from the boundary. However, if the reader's power has achieved to the maximum value $\max P_w$, n_b is still less than n_ε, which indicates that most of the *interference tags* are far away from S. Then, the reader stops the process and gets the optimal power $P_w^* = \max P_w$. After that, the antenna rotates towards the center of S for *power stepping* and tag identification.

Algorithm 1. PID: Establishing the Boundary

Input: The specified area S
Determine the boundary S_b of S by the 3D camera, and calculate d_b and d_s.
The antenna rotates to S_b with $\varphi = arccos(\frac{d_s}{d_b})$.
$P_{wb} = P_{w_{min}}(90°, d_b)$, $P_w = P_{wb}$, $n_b = 0$.
while $n_b < n_\varepsilon$ *and* $P_w < \max P_w$ **do**
  Collect tag IDs with P_w and get n_b responses.
  if $P_w = \max P_w$ *and* $n_b < n_\varepsilon$ **then**
  $P_w^* = \max P_w$, Return.
  $P_w = \min(P_w + \Delta P_w, \max P_w)$.
Get the tag IDs $N_b = \{ID_1, ID_2, \ldots, ID_{n_b}\}$.
Output: Tag IDs in the boundary: N_b

6.1.3 Power Stepping

If P_w^* has not been determined, the reader will adjust the power through power stepping. Firstly, the reader chooses an initial power $P_{ws} = P_{w_{min}}(\theta_r, d)$ according to φ and d_b, where $\theta_r = 90° - \varphi$ and $d = d_b$. It is a critical value in theory, whose interrogation region just achieves the boundary of S. However, as shown in Fig. 3e, the tag size can affect the effective interrogation region; P_{ws} may not be the most reasonable power. Thus, we properly adjust the power by checking the tag IDs in N_b, as shown in Algorithm 2.

Algorithm 2. PID: Power Stepping

Input: Tag IDs in N_b
$P_{ws} = P_{w_{min}}(\theta_r, d) = P_{w_{min}}(90° - \varphi, d_b)$,
$P_w = P_{ws}$.
Check the tag IDs in N_b and get n_c responses N_c.
if $\frac{n_c}{n_b} = \delta$ **then** $P_w^* = P_{ws}$.
if $\frac{n_c}{n_b} > \delta$ **then**
  while $P_w > \min P_w$ **do**
    $P_w = \max(P_w - \Delta P_w, \min P_w)$.
    Check IDs in N_c, get Δn_c responses,
    $n_c = \Delta n_c$.
    if $\frac{n_c}{n_b} \leq \delta$ **then** $P_w^* = P_w$, Return.
  if $P_w = \min P_w$ **then** $P_w^* = \min P_w$, Return.
if $\frac{n_c}{n_b} < \delta$ **then**
  while $P_w < \max P_w$ **do**
    $P_w = \min(P_w + \Delta P_w, \max P_w)$.
    Check IDs in $N_b - N_c$, get Δn_c responses,
    $n_c = n_c + \Delta n_c$.
    if $\frac{n_c}{n_b} \geq \delta$ **then** $P_w^* = P_w$, Return.
  if $P_w = \max P_w$ **then** $P_w^* = \max P_w$, Return.
Output: The optimal power P_w^*

In the commercial RFID systems, the reader (e.g., Alien-9900+) selects a specified tag by setting the mask equal to

TABLE 2
Upper Bound n_u

N	20	60	100	140	180	220
n_u	2	4	7	9	11	12

the tag ID. If the tag gives response, the reader gets a non-empty slot. Otherwise, it gets an empty slot. The reader checks all the IDs in N_b and gets n_c responses N_c. Obviously, $n_c \leq n_b$. When $\frac{n_c}{n_b} = \delta$, the interrogation region just achieves the boundary of S. The corresponding power is the optimal power P_w^*. However, if $\frac{n_c}{n_b} > \delta$, the reader reduces the power by ΔP_w and checks the verified tag IDs in N_c. If a tag does not give response, the reader removes it from N_c. It repeats the above process until $\frac{n_c}{n_b} \leq \delta$ and gets the optimal power P_w^*. On the contrary, if $\frac{n_c}{n_b} < \delta$, the reader increases P_w by ΔP_w and checks the unverified tag IDs in $N_b - N_c = \{ID_i \mid ID_i \in N_b \text{ and } ID_i \notin N_c\}$. If the tag gives response, the reader adds the ID into N_c. It repeats the process until $\frac{n_c}{n_b} \geq \delta$ and gets the optimal power P_w^*. In the following process, the reader uses P_w^* to identify the *target tags*.

6.2 Shooting Process

In this process, the reader collects the tag IDs in S. The reader's power is equal to P_w^* and we use frame slotted ALOHA (FSA) protocol to identify the tags. FSA is a popular anti-collision protocol. In FSA, the reader first broadcasts a number f, which specifies the following frame size. After receiving f, each tag selects $h(ID) \bmod f$ as its slot number, where h is a hash function. If none of the tags respond in a slot, the reader closes the slot immediately. If only one tag responds in a slot, the reader successfully receives the tag ID. If multiple tags respond simultaneously, a collision occurs, and the involved tags will be acknowledged to restart in the next frame. The similar process repeats until no tags respond in the frame. The collected IDs are considered as the *target tag IDs*.

6.3 Performance Analysis

In order to definitely describe the boundary S_b, PID needs to steadily get at least n_ε interference tag IDs, and n_b satisfies $n_b \geq n_\varepsilon$. That is to say, n_ε is the minimum number of *interference tags* needed to establish the boundary of the area S. In the realistic environment, some tags may not be identified by the reader steadily. If the power arriving at a tag is approximate to the minimum power to activate it, the tag may respond to the reader or keep silent at random, which will affect the judgement of the boundary. Therefore, we measure the value of n_ε with a different tag size $|N|$ in the realistic environments, as shown in Table 2. Based on Table 2, we can conclude that tag size $|N|$ has a little effect on n_ε, which is usually very small. Therefore, in order to definitely get enough tag IDs in S_b, we set $n_\varepsilon = 15$ by default, while considering the stability and time efficiency.

In regard to δ, it affects the *misreading ratio*. The smaller the value of δ, the lower the *misreading ratio*, the smaller the execution time. However, the larger the value of δ, the larger the value of *coverage ratio*. Considering the constraint of coverage ratio ρ and time efficiency, we set $\delta = \alpha$. When
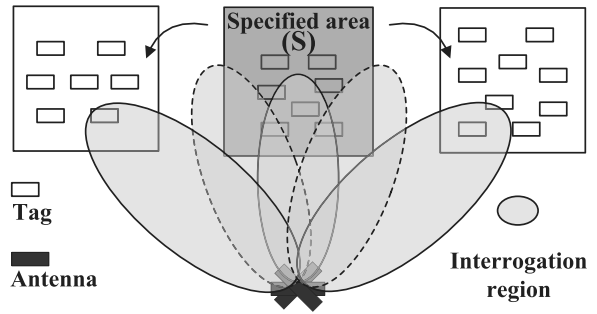

Fig. 7. Identify the tags in S without any auxiliary equipment.

$\frac{n_c}{n_b} = \delta = \alpha$, we consider that the interrogation region only achieves the boundary, and the coverage ratio ρ satisfies $\rho \geq \alpha$. At this time, the reader gets the optimal power

$$P_w^* = P_{ws} + k_c \times \Delta P_w, \quad k_c \in \mathbb{Z}. \qquad (3)$$

Here, we set $\Delta P_w = 1 \, \text{dBm}$, which is achievable by most of the commercial readers [30]. k_c represents the number of steps needed to update the reader's power, and k_c is adaptively determined in the identification process.

In PID, when the rotation angle is determined, the antenna rotates to the target direction immediately. The time for rotating the antenna can be neglected when compared to the identification time. Based on the above analysis, we can estimate the lower bound of the execution time T_l for PID as follows:

$$T_l = \sum_{i=0}^{i=k_b} (e \cdot n_b(i) \cdot \tau) + \sum_{j=0}^{j=k_c} (n_c(j) \cdot \tau) + e \cdot n \cdot \tau. \qquad (4)$$

Here, $n_b(i)$ is the number of tags identified from the boundary in the ith step, $n_c(j)$ is the number of tags identified in S_b in jth step, n is the number of *target tags* checked in the shooting process, τ is the time for a slot, and e is the base of the natural logarithm. From Eq. (4), we can find that the numbers k_b, k_c, n affect T_l, which is related to the reader's power. Thus, choosing the optimal power P_w^* is essential to the problem, as shown in Algorithm 2.

7 PHOTOGRAPHY BASED IDENTIFICATION WITH ANGLE ROTATION

In PID, a 3D camera is used in the focusing process. However, in some environments, the 3D camera can not work well (e.g., in a dark space). Besides, considering the cost savings, it may not be used. Therefore, identifying the *target tags* without the auxiliary equipment is important. For this problem, we propose a solution called Photography based tag Identification with Angle rotation (PIA). It also consists of the *Focusing Process* and *Shooting Process*. The only difference between PID and PIA is how to determine the boundary of S. Therefore, we only describe how to find the boundary in PIA, while ignoring the others.

7.1 PIA

Without the 3D camera, PIA cannot calculate any distance; it explores the boundary by rotating the antenna, as shown in Fig. 7. Firstly, the application appoints S and the antenna rotates towards S. Then the reader sets its initial power

equal to the minimum power $\min P_w$ and identifies n_s tags in S. If $n_s < n_\varepsilon$, the reader repeatedly increases the power by ΔP_w and identifies the tags until $n_s \geq n_\varepsilon$, the identified *target tags* are $N_s = \{ID_1, ID_2, \ldots, ID_{n_s}\}$. If $P_w = \max P_w$, PIA gets $P_w^* = \max P_w$. Otherwise, the antenna rotates away from S to get the interference tag IDs in the boundary, as shown in Algorithm 3.

Algorithm 3. PIA: Exploring the Boundary

Input: The specified area S
$P_w = \min P_w, n_s = 0, n_l = 0, \Delta \theta_{r_l} = 0°$.
while $n_s < n_\varepsilon$ and $P_w < \max P_w$ **do**
   Get n_s tag IDs, $P_w = \min(P_w + \Delta P_w, \max P_w)$.
if $P_w = \max P_w$ **then** $P_w^* = \max P_w$, Return.
Get tag IDs $N_s = \{ID_1, ID_2 \ldots, ID_{n_s}\}$.
$i = 1$.
while $n_l < n_\varepsilon$ and $\Delta \theta_{r_l} < 90°$ **do**
   The antenna rotates to the left, the accumulative rotation
   angle is $\Delta \theta_{r_l} = \min(\Delta \theta_{r_l} + \Delta \theta_r, 90°)$.
   while $P_w < \max P_w$ **do**
      Δn_{s_i} tag IDs in N_s disappear, $n_{s_i} = n_s - \Delta n_{s_i}$.
      Get n_l tag IDs N_l not in S.
      if $n_l \geq n_\varepsilon$ **then** Break.
      if $n_{s_i} < n_s$ **then**
         if $i > 1$ and $\Delta n_{s_i} < \Delta n_{s_{i-1}}$ **then** Break.
         $P_w = \min(P_w + \Delta P_w, \max P_w)$.
      else Break.
      $i = i + 1$.
$P_{wl} = P_w, N_b = N_l$.
The antenna rotates to the right in $[0 \text{ degree}, \Delta \theta_{r_l}]$, gets N_r and P_{wr}, it rotates $\Delta \theta_{rr}$ degree.
if $\Delta \theta_{r_l} = \Delta \theta_{rr}$ and $P_{wl} = P_{wr}$ **then** $N_b = N_l \cup N_r$.
else if $\Delta \theta_{r_l} = \Delta \theta_{rr}$ and $P_{wl} > P_{wr}$ **then** $N_b = N_r$.
else if $\Delta \theta_{r_l} > \Delta \theta_{rr}$ **then** $N_b = N_r$.
Output: Tag IDs in the boundary : N_b

When the antenna rotates to another direction (called *left*), the identified tags in S decreases. As shown in Algorithm 3, the radiation angle decreases by $\Delta \theta_r$. In the ith step, Δn_{s_i} tags disappear from S, the number of identified tags in S is n_{s_i}. At the same time, the reader gets n_l tag IDs out of S, and they are considered as the tag IDs from the boundary. If $n_l \geq n_\varepsilon$, the reader collects enough tag IDs $N_l = \{ID'_1, ID'_2, \ldots, ID'_{n_l}\}$ from the boundary. Otherwise, it increases the power by ΔP_w. Each time, it should make sure that $n_{s_i} < n_s$ and $\Delta n_{s_i} \geq \Delta n_{s_{i-1}}$, which indicates that the new identified tag IDs are not from the area S. Otherwise, the antenna keeps rotating away from S. PIA repeats the above process until $n_l \geq n_\varepsilon$. Then, the antenna has rotated $\Delta \theta_{r_l}$ degrees. At this time, the ending power of the reader is P_{wl}. After that, the antenna rotates to the opposite direction (*right*) and works in the same way. It rotates $\Delta \theta_{rr}$ degrees to the right side and the ending power of the reader is P_{wr}. If $\Delta \theta_{rr} > \Delta \theta_{r_l}$, it indicates that the boundary on the right side is farther than that of the left one, then the reader terminates the process. Otherwise, it obtains $N_r = \{ID''_1, ID''_2, \ldots, ID''_{n_r}\}$. The reader compares $\Delta \theta_{r_l}, \Delta \theta_{rr}$ and P_{wl}, P_{wr} to find the nearer boundary, and gets the new set N_b of interference tags. If $\Delta \theta_{r_l} = \Delta \theta_{rr}$ and $P_{wl} = P_{wr}$, $N_b = N_l \cup N_r$. If $\Delta \theta_{r_l} = \Delta \theta_{rr}$, while $P_{wl} > P_{wr}$, $N_b = N_r$. Besides, if $\Delta \theta_{r_l} > \Delta \theta_{rr}$, $N_b = N_r$. Otherwise, $N_b = N_l$. Here, N_b is used for

power stepping. If P_w^* has not been determined, PIA utilizes the ending power P_{wl}, P_{wr} to determine the initial power P_{ws}. If $N_b = N_l$, $P_{ws} = P_{wl}$. Otherwise, $P_{ws} = P_{wr}$. P_{ws} is used for power stepping, which is described in Algorithm 2.

The values of parameters in PIA are equal to those in PID. In regard to $\Delta \theta_r$ in PIA, we set $\Delta \theta_r = 30°$. Based on Fig. 3a, when $\theta_r \in [75°, 90°]$, the reader undoubtedly has good performance. Therefore, when $\Delta \theta_r = 30°$, each tag can be requested in the center of the interrogation region with $\theta_r \in [75°, 90°]$. PIA does not identify the tags while the antenna is rotating. This is because the reader cannot determine where the identified tags are located, when the antenna is rotating. Therefore, PIA rotates to the next direction immediately as PID does, then it identifies the tags.

7.2 Comparison of PID and PIA

We compare PID and PIA in the following aspects:

- *System equipment*. PID uses an auxiliary equipment (i.e., a 3D camera), while PIA does not need any auxiliary equipment.
- *Performance comparison*. With the 3D camera, PID can quickly focus on the specified area and reduce the execution time. PIA needs to rotate the antenna to find the specified area, it often needs more execution time and identifies more interference tags.
- *Application environment*. By using the 3D camera, PID recognizes the specified area by the RGB camera and measures distance by the 3D depth sensor. In the environments like dark spaces, the RGB camera can not work well, thus PID can not work well. While PIA will not be affected by the surroundings and can work well in different environments.

8 EXTENSION FOR TAG IDENTIFICATION TOWARDS TWO-DIMENSIONAL SPACE

In Section 3, the *target tags* and the *interference tags* are mainly located in one-dimensional space (Our previous conference version [31] focuses on this problem.). However, in some applications, the objects may be located around the *target tags* in two-dimensional space, as shown in Fig. 8.

In this case, PID can still use the 3D camera to distinguish the target tags and interference tags. Unfortunately, PIA may not work well, because it mainly identifies the *interference tags* in one-dimensional space (see Fig. 7). It may not find the boundary appropriately in two-dimensional space. Thus we improve PIA as the Enhanced Photography based Identification with Angle rotation (EPIA) to identify the *target tags* in two-dimensional space.

In EPIA, the reader identifies some target tags N_s as PIA does. Then, it begins to identify the *interference tags* in the boundary S_b around the specified area S, as shown in Fig. 8. The antenna first randomly selects a direction to identify some tags N_{b1} from the boundary, as shown in Algorithm 4. Then, it rotates $\Delta \theta_{rc}$ in clockwise direction in order to identify other tags around the boundary, aiming to find the *interference tags* closest to the *target tags*, as shown in Fig. 8. In the newly-selected direction, it identifies the *interference tags* as PIA does. When the antenna has finished identifying the tags around the specified S, it will select the *interference tags* with the smallest rotation angle value $\Delta \theta_{rk}$, $k \in [1, \lceil \frac{360°}{\Delta \theta_{rc}} \rceil]$,
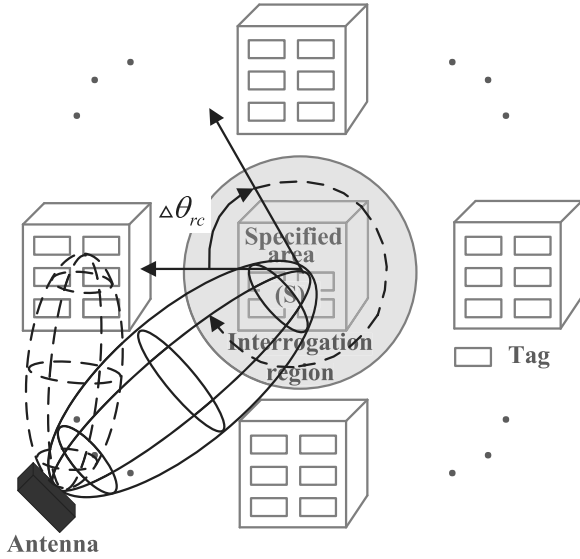
Fig. 8. Identify the tags in the specified area in two-dimensional space.

Fig. 9. Tags located at different depths.

which means the identified tag sets $\{N_{bk}\}$ are closest to the *target tags*. Then, the reader selects one set N_{bk} which is identified with the smallest power P_{wk} from $\{N_{bk}\}$, and uses N_{bk} as the *interference tags*, which will be used for power stepping as PIA does. Similarly, EPIA selects this smallest ending power P_{wk} as the initial power P_{ws} for power steeping, which is described in Algorithm 2.

Algorithm 4. EPIA: Exploring the Boundary in Two-Dimensional Space

---

Input: The specified area S
$P_w = \min P_w$, $n_s = 0$, $\theta_c = 0°$.
while $n_s < n_\varepsilon$ *and* $P_w < \max P_w$ **do**
  Get n_s tag IDs N_s,
  $P_w = \min(P_w + \Delta P_w, \max P_w)$.
if $P_w = \max P_w$ **then** $P_w^* = \max P_w$, Return.
The antenna randomly selects a direction to identify interference tags, $k = 1$, $\Delta\theta_{min} = 90°$.
while $\theta_c \in [0°, 360°)$ **do**
  $i = 1$, $n_k = 0$, $\Delta\theta_{rk} = 0°$.
  while $n_k < n_\varepsilon$ *and* $\Delta\theta_{rk} < \Delta\theta_{min}$ **do**
    The antenna rotates away from the target tags,
    the accumulative rotation angle is
    $\Delta\theta_{rk} = \min(\Delta\theta_{rk} + \Delta\theta_r, \Delta\theta_{min})$.
    while $P_w < \max P_w$ **do**
      Δn_{s_i} tag IDs in N_s disappear,
      $n_{s_i} = n_s - \Delta n_{s_i}$.
      Get n_k tag IDs N_{bk} not is S.
      if $n_k \geq n_\varepsilon$ **then** Break.
      if $n_{s_i} < n_s$ **then**
        if $i > 1$ *and* $\Delta n_{s_i} < \Delta n_{s_{i-1}}$ **then**
          Break.
        $P_w = \min(P_w + \Delta P_w, \max P_w)$.
      else Break.
    $i = i + 1$.
    $P_{wk} = P_w$.
    if $\Delta\theta_{rk} < \Delta\theta_{min}$ **then** $\Delta\theta_{min} = \Delta\theta_{rk}$.
  $\theta_c = \theta_c + \Delta\theta_{rc}$, $k = k + 1$.
For the sets $\{N_{bk}\}$ satisfying $\Delta\theta_{rk} = \Delta\theta_{min}$, select one N_{bk} with the smallest P_{wk}.
$N_b = N_{bk}$.
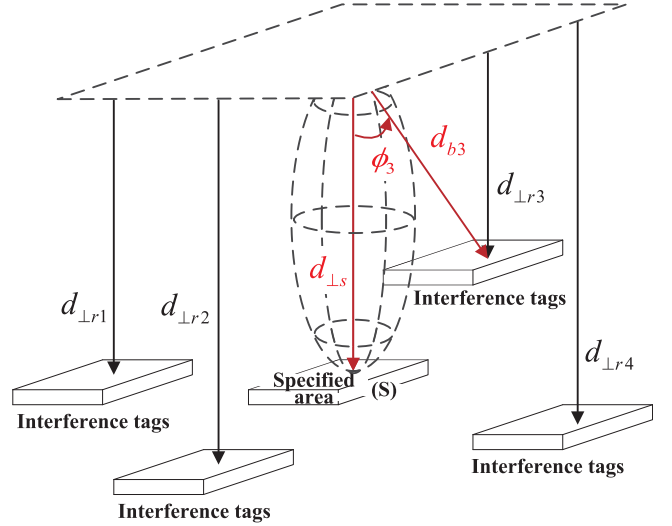**Output:** Tag IDs in the boundary : N_b

---

In order to find the area containing interference tags, EPIA rotates the antenna around the specified area S. We use $\Delta\theta_{rc}$ to divide the boundary into different regions, as shown in Fig. 8. According to Fig. 3a in Section 4, when the rotation angle $\theta_r \in [60°, 90°]$, the reader has better performance to identify the tags. Therefore, we set $\Delta\theta_{rc} = 60°$, in order to make sure that each region of the boundary can be located in the reader's effective scanning range. However, when the direction is fixed, the reader identifies the tags as PIA does. When identifying the tags in one direction, the antenna rotates away from the *target tags* by $\Delta\theta_r = 30°$ to identify the *interference tags* as PIA does. In this way, the tags to be identified are always located in the center of the interrogation region. It means that $\theta_r \in [75°, 90°]$, where the reader will undoubtedly have good performance for tag identification. The difference between the value of $\Delta\theta_{rc}$ and $\Delta\theta_r$ lies in that $\Delta\theta_{rc}$ is only used to divide the boundary, while $\Delta\theta_r$ is used to identify the tags.

9 DISCUSSION FOR TAG IDENTIFICATION TOWARDS MORE COMPLEX ENVIRONMENTS

In the above sections, the *target tags* and the *interference tags* are mainly located at the same depth. However, in more complex environments, the objects may be located at different depths. As shown in Fig. 9, the vertical distance between the *target tags* and the antenna is $d_{\perp s}$, while the vertical distance between the *interference tags* and the antenna are $d_{\perp r1}, d_{\perp r2}, d_{\perp r3}, d_{\perp r4}$, respectively. The value of $d_{\perp s}$ and $d_{\perp ri}(i \in [1, 4])$ may be different.

At this time, the rotation angle φ of the antenna cannot be calculated by 3D camera in the way described in Section 6.1.2. For example, the 3D camera can calculate the distances $d_{\perp s}$ and d_{b3}, while $\varphi_3 \neq arccos(\frac{d_{\perp s}}{d_{b3}})$, because $d_{\perp s} \neq d_{\perp r3}$. PID can not work well in such an environment. Fortunately, we can use EPIA to explore the boundary of the specified area S by rotating the antenna. However, if the $d_{\perp ri}(i \in [1, 4])$ is much smaller than $d_{\perp s}$, more interference tags will be identified. At this time, we can try to adjust the placement of the objects or antenna, aiming to reduce the depth difference among the tags. Then, the reader uses EPIA to identify the *target tags*.
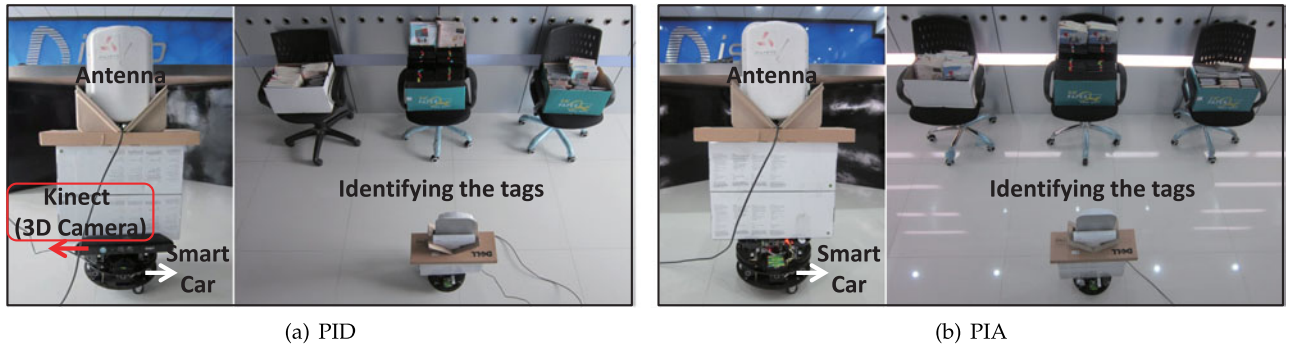
(a) PID   **(b) PIA**

Fig. 10. System prototypes work in the realistic environments.

10 PERFORMANCE EVALUATION

We evaluate the performance of each solution in the realistic environments. The experimental facilities are the same as those used in the observations. The *execution time*, *coverage ratio*, and *misreading ratio* are used for performance metrics.

In the experiments, each book is attached with an RFID tag, and the tag ID is 96 bits. The books are randomly deployed in three boxes and the distribution of the tag IDs are unknown. Each box is placed on a tablet chair with a height of 0.5 m, as shown in Fig. 10. PID uses a 3D camera, while PIA does not. The antenna is deployed on the smart car, which is controlled by the program and can rotate with the antenna flexibly. The antenna faces towards the tags to be identified. The specified area here is the center box, which is the *target box*, while the other two boxes are *interference boxes*. The distance between the target box and the antenna is d. The minimum distance between the interference box and the target box is l. s and u respectively represent the number of target tags (in target box) and the number of interference tags (in interference boxes). We vary the values of d, l, s, u to evaluate the performance of each solution. We set $d = 1\,\mathrm{m}$, $l = 1\,\mathrm{m}$, $s = 80$, $u = 70$ by default.

10.1 Upper Bound of α

As mentioned in Section 3.2, when the distance d, and the number of tags n are fixed, we can determine the value of α. In Table 3, we give the upper bound of α under different conditions. We set $\alpha = 60\%$ for the following experiments by default.

10.2 Coverage Ratio ρ Constraint

We first investigate the coverage ratio ρ of each solution, as shown in Fig. 11. We can observe that scanning with the minimum power cannot achieve the requirement of coverage ratio ($\alpha = 60\%$). This is because the power is too small to activate the majority of the tags. When we identify the tags with the maximum power (MaxPw) or our proposed solutions (PID and PIA), the coverage ratios are all larger

TABLE 3
Upper Bound of α

n \ d (m)	0.5	1.0	1.5
40	100%	100%	90%
80	95%	85%	65%
120	89%	81%	63%

than 60 percent ($\rho \geq \alpha$), which satisfies the requirement. As mentioned in Section 3.2, the coverage ratio must be satisfied. Therefore, the solution MinPw is invalid and we ignore it in the following comparisons.

10.3 Execution Time T

Fig. 12 shows the execution time of each solution. Our solutions PID and PIA have better performances than MaxPw. This is because PID and PIA only focus on the *target tags* in S. MaxPw identifies all the tags in the interrogation region, including a lot of *interference tags*. Usually, PID has a better performance than PIA, due to the use of a 3D camera. In Figs. 12a and 12b, the difference in execution time between PID, PIA and MaxPw is small. This is because the tag size is relatively small. When the tag size becomes large, our proposed solutions become more efficient. When $s = 120$, PID reduces the execution time by 44 percent compared to MaxPw, as shown in Fig. 12c. When $u = 270$, PID even can reduce the execution time by 85.6 percent compared to MaxPw, as shown in Fig. 12d.
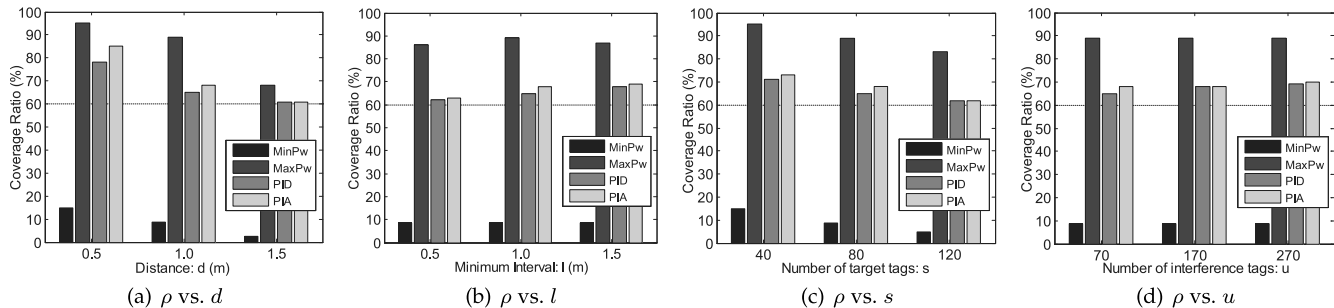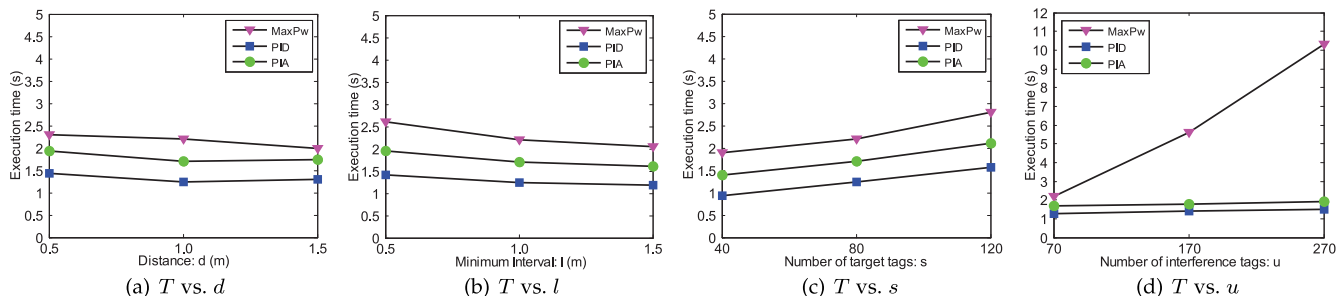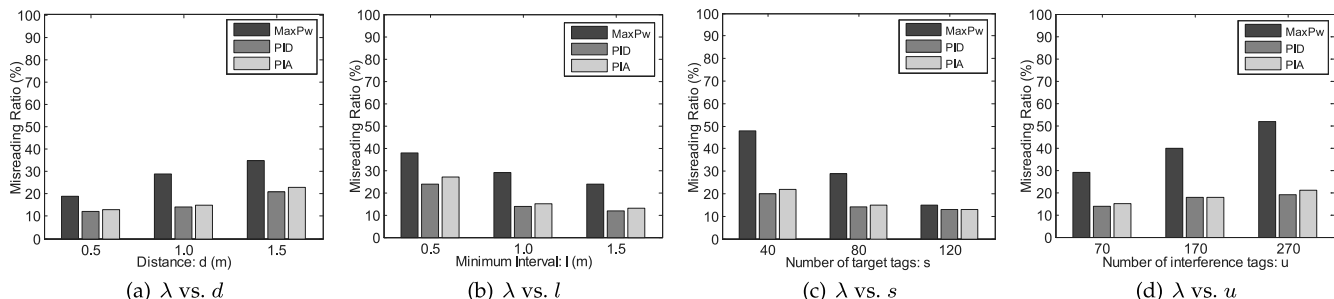
10.4 Misreading Ratio λ

In Section 3.2, we analyze that the execution time is related to the misreading ratio. Fig. 13 shows the misreading ratio of each solution. Our solutions PID and PIA have lower misreading ratios than MaxPw. This is because PID and PIA use the optimal powers instead of the maximum one (30.7 dBm). PID and PIA mainly focus on the *target tags*, while avoiding identifying the *interference tags*.

When we change α, our solutions can also work well. For example, when $d = 1\,\mathrm{m}$, $l = 1\,\mathrm{m}$, $s = 80$, $u = 70$, we set $\alpha = 80\%$. The coverage ratio of MaxPw, PID, PIA is respectively equal to 89, 82.5, 86 percent, which satisfy $\rho \geq \alpha$. The execution time of MaxPw, PID, PIA is respectively equal to 2.2, 1.45, 2.0 s. Our solutions outperform the baseline solutions.

10.5 Using Different Types of Tags

We conduct the experiment with Alien-9640 tags, Alien-9654 tags, and Impinj H47 tags. The tag cardinality of each type is almost the same. We randomly mix these tags together in interference tags and target tags. We vary the minimal distance l between target tags and interference tags in the experiments. As shown in Fig. 14, the mixed tags have a little effect on the reading performance, which is coincident with Fig. 13l. The performance of each solution is similar to that shown in Figs. 11b, 12b, 13b. When $l = 1\mathrm{m}$,

Fig. 11. $\alpha = 60\%$, coverage ratio.

Fig. 12. $\alpha = 60\%$, execution time.

Fig. 13. $\alpha = 60\%$, misreading ratio.
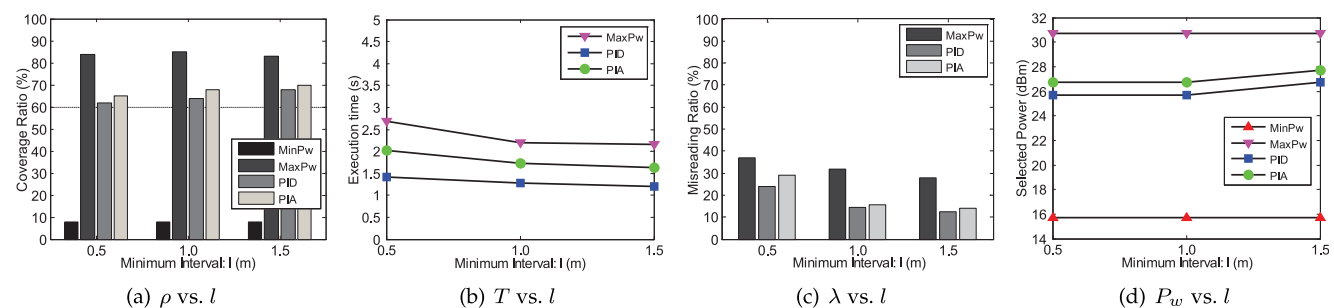
Fig. 14. $\alpha = 60\%$, tag identification with different types of tags.

PID reduces the execution time by 42 percent compared to MaxPw. This is because our solutions try to select the optimal power to identify the tags instead of using the default power, as shown in Fig. 14d.

10.6 Varying the Placement of Tags

We make the interference tags face towards the antenna, while rotating the targets tags by 45 degree along the x-axis. We vary the minimal distance l between target tags and interference tags in the experiments. As shown in Fig. 15, the placement of tags have some effect on the performance

of each solution. However, our solutions PID and PIA still have better performance than the baseline solutions. When the power is large enough, the reader can identify the target tags. Because the target tags are located in the major interrogation region, while the interference tags are mostly in minor interrogation region, as described in Fig. 4b. Both PID and PIA can achieve the requirement of coverage ratio ($\alpha = 60\%$), as shown in Fig. 15a. When $l = 1$m, PID reduces the execution time by 51 percent compared to MaxPw, as shown in Fig. 15b. PID and PIA identify fewer interference tags than MaxPw does, as shown in Fig. 15c. This is because
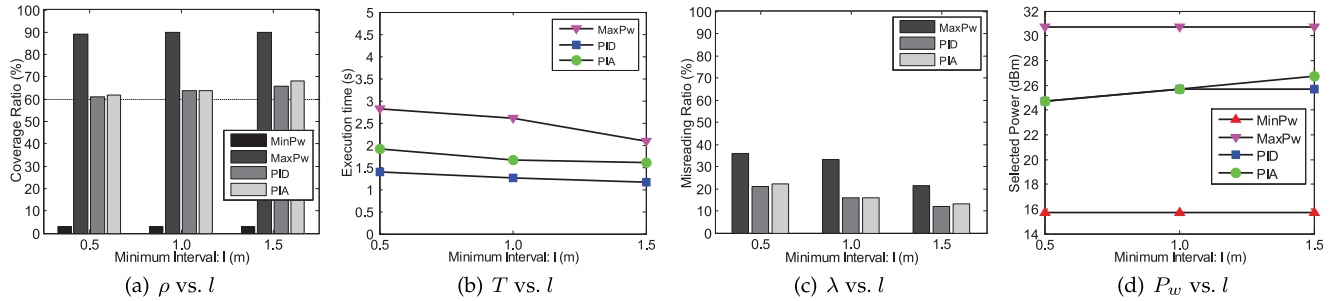
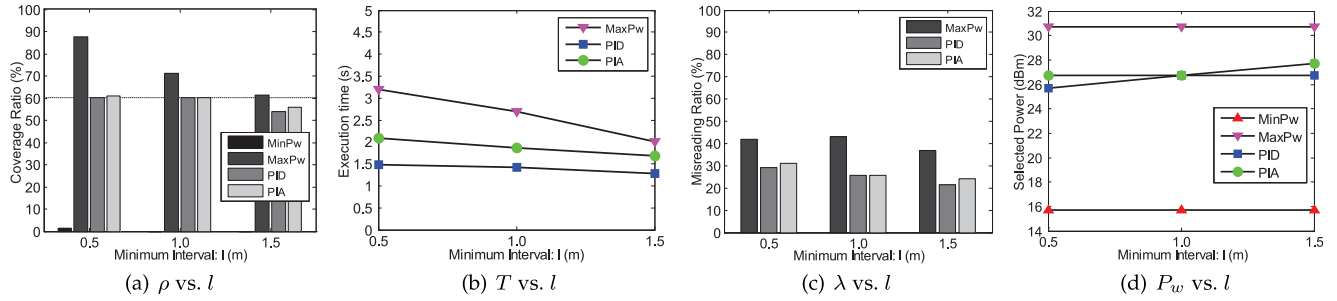Fig. 15. $\alpha = 60\%$, tag identification with different tag placement.

(a) ρ vs. l (b) T vs. l (c) λ vs. l (d) P_w vs. l

Fig. 16. $\alpha = 60\%$, tag identification with target tags in left area.
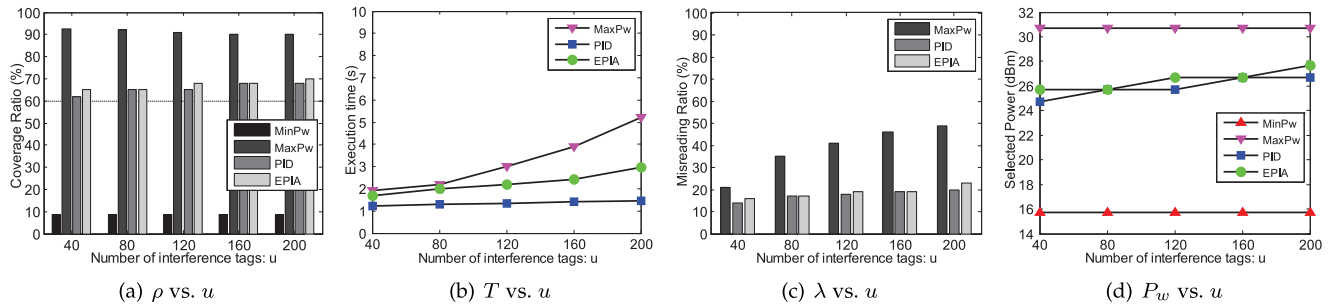
(a) ρ vs. l (b) T vs. l (c) λ vs. l (d) P_w vs. l

Fig. 17. $\alpha = 60\%$, tag identification towards two-dimensional space.

(a) ρ vs. u (b) T vs. u (c) λ vs. u (d) P_w vs. u

our solutions try to select the optimal power to identify the tags, as shown in Fig. 15d.

10.7 Changing the Location of Target Tags

In this experiment, we change the left area in Fig. 1 as the specified area. The interference tags in the center area are in front of the antenna. We vary the minimal distance l between target tags and interference tags. The distance between the target tags and the antenna is farther than that between the interference tags and the antenna. Therefore, the coverage ratio decreases, while the misreading ratio increases, as shown in Figs. 16a and 16c. However, based on Fig. 4b, the target tags are in the major interrogation region, while the interference tags are mostly in minor interrogation region. Due to the different performances in major / minor interrogation regions, our solutions can basically satisfy the requirement $\rho \geq \alpha$, as shown in Fig. 16a. When $l = 1.5$ m, the coverage ratios of PID and PIA are a little less than the requirement. Because the distance between the target tags and the antenna is about 1.8 m, which is too large, according to Table 3. Even using the maximal power, the coverage ratio is only about 61 percent. In such a scenario, it is appropriate to decrease the requirement of α. Nevertheless, our proposed solutions still have

better performance than the baseline solutions. When $l = 1$m, PID reduces the execution time by 47 percent compared to MaxPw, as shown in Fig. 16b. PID and PIA do not identify too many interference tags as MaxPw does, as shown in Fig. 16c. Because our solutions try to select the optimal power to identify the target tags, as shown in Fig. 16d.

If we want to further improve the coverage ratio and reduce the misreading ratio, we can use multiple readers [32], [33] to joint identify the target tags. For example, the target tags are located in the left side of antenna $A1$, while in the right side of antenna $A2$. Then, we can take the intersection of the identified tags from $A1$ and $A2$ as the target tags, while eliminating the other tags. In future, we will consider how to schedule the multiple readers and improve the efficiency of our solutions with multiple readers.

10.8 Extension for Tag Identification Towards Two-Dimensional Space

In order to evaluate the performance of our solutions in two-dimensional space, we conduct the following experiment in the bookshelf. We deploy the books (tags) as Fig. 8 shows. The books located in the center of the bookshelf are *target tags*, while the tags around the target tags are *interference tags*. We vary the number of interference tags u to in the

experiments. Based on Fig. 17a, both PID and EPIA can achieve the requirement of coverage ratio ($\alpha = 60\%$). Besides, our solutions PID and EPIA have better performance than the baseline solution. When $u = 200$, EPIA reduces the execution time by 43 percent compared to MaxPw, as shown in Fig. 17b. Besides, PID and EPIA have lower misreading ratios, as shown in Fig. 17c. This is because PID and EPIA try to select the optimal power to focus on the specified area, while avoiding identifying the *interference tags*. The optimal power is usually larger than the minimum power and smaller than the maximum (default) power, as shown in 17d.

11 CONCLUSION

In this paper, we investigate the problem of identifying the tags in the specified area. We conduct extensive experiments on the commodity RFID system in real environments and present two efficient solutions, PID and PIA. They work in a similar way of picture-taking in an auto-focus camera. They first focus on the specified area and then identify the *target tags*. Furthermore, we improve the proposed solutions to make them work well in more complex environments. The realistic experiments show that our solutions outperform the baseline solutions.

REFERENCES

[1] J. Myung, W. Lee, and J. Srivastava, "Adaptive binary splitting for efficient RFID tag anti-collision," *IEEE Commun. Lett.*, vol. 10, no. 3, pp. 144–146, Mar. 2006.

[2] L. Pan and H. Wu, "Smart trend-traversal protocol for RFID tag arbitration," *IEEE Trans. Wireless Commun.*, vol. 10, no. 11, pp. 3565–3569, Nov. 2011.

[3] T. L. Porta, G. Maselli, and C. Petrioli, "Anti-collision protocols for single-reader RFID systems: Temporal analysis and optimization," *IEEE Trans. Mobile Comput.*, vol. 10, no. 2, pp. 267–279, Feb. 2011.

[4] M. Shahzad and A. Liu, "Probabilistic optimal tree hopping for RFID identification," in *Proc. ACM SIGMETRICS/Int. Conf. Measurement Modeling Comput. Syst.*, 2014, pp. 293–304.

[5] H. Vogt, "Efficient object identification with passive RFID tags," in *Proc. 1st Int. Conf. Pervasive Comput.*, 2002, pp. 98–113.

[6] Y. Maguire and R. Pappu, "An optimal q-algorithm for the ISO 18000-6c RFID protocol," *IEEE Trans. Autom. Sci. Eng.*, vol. 6, no. 1, pp. 16–24, Jan. 2009.

[7] B. Zhen, M. Kobayashi, and M. Shimuzu, "Framed aloha for multiple RFID objects identification," *IEICE Trans. Commun.*, vol. E80-B, no. 3, pp. 991–999, Mar. 2005.

[8] L. Xie, B. Sheng, C. Tan, H. Han, Q. Li, and D. Chen, "Efficient tag identification in mobile RFID systems," in *Proc. IEEE INFOCOM*, 2010, pp. 1–9.

[9] C. Tan, B. Sheng, and Q. Li, "Efficient techniques for monitoring missing RFID tags," *IEEE Trans. Wireless Commun.*, vol. 9, no. 6, pp. 1882–1889, Jun. 2010.

[10] W. Luo, S. Chen, T. Li, and Y. Qiao, "Probabilistic missing-tag detection and energy-time tradeoff in large-scale RFID systems," in *Proc. ACM MobiHoc*, 2012, pp. 95–104.

[11] X. Liu, K. Li, G. Min, Y. Shen, A. Liu, and W. Qu, "Completely pinpointing the missing RFID tags in a time-efficient way," *IEEE Trans. Comput.*, vol. 64, no. 1, pp. 87–96, Jan. 2015.

[12] T. Li, S. Chen, and Y. Ling, "Efficient protocols for identifying the missing tags in a large RFID system," *IEEE/ACM Trans. Netw.*, vol. 21, no. 6, pp. 1974–1987, Dec. 2013.

[13] Y. Zheng and M. Li, "P-MTI: Physical-layer missing tag identification via compressive sensing," in *Proc. IEEE INFOCOM*, 2013, pp. 917–925.

[14] X. Liu, K. Li, G. Min, Y. Shen, A. X. Liu, and W. Qu, "A multiple hashing approach to complete identification of missing RFID tags," *IEEE Trans. Commun.*, vol. 62, no. 3, pp. 1046–1057, Mar. 2014.

[15] X. Liu, B. Xiao, S. Zhang, and K. Bu, "Unknown tag identification in large RFID systems: An efficient and complete solution," *IEEE Trans. Parallel Distrib. Syst.*, vol. 26, no. 6, pp. 1775–1788, Jun. 2015.

[16] X. Liu, K. Li, G. Min, K. Lin, B. Xiao, Y. Shen, and W. Qu, "Efficient unknown tag identification protocols in large-scale RFID systems," *IEEE Trans. Parallel Distrib. Syst.*, vol. 25, no. 12, pp. 3145–3155, Dec. 2014.

[17] H. Yue, C. Zhang, M. Pan, Y. Fang, , and S. Chen, "Unknown-target information collection protocol in sensor-enabled RFID systems," *IEEE/ACM Trans. Netw.*, vol. 22, no. 4, pp. 1164–1175, Aug. 2014.

[18] Y. Zheng and M. Li, "Fast tag searching protocol for large-scale RFID systems," in *Proc. IEEE Int. Conf. Netw. Protocols*, 2011, pp. 363–372.

[19] Y. Qiao, S. Chen, T. Li, and S. Chen, "Energy-efficient polling protocols in RFID systems," in *Proc. 12th ACM Int. Symp. Mobile Ad Hoc Netw. Comput.*, 2011, pp. 226–235.

[20] H. Yue, C. Zhang, M. Pan, Y. Fang, and S. Chen, "A time-efficient information collection protocol for large-scale RFID systems," in *Proc. IEEE INFOCOM*, 2012, pp. 2158–2166.

[21] H. Han, B. Sheng, C. C. Tan, Q. Li, W. Mao, and S. Lu, "Counting RFID tags efficiently and anonymously," in *Proc. IEEE INFOCOM*, 2010, pp. 1–9.

[22] M. Kodialam and T. Nandagopal, "Fast and reliable estimation schemes in RFID systems," in *Proc. 12th Annu. Int. Conf. Mobile Comput. Netw.*, 2006, pp. 322–333.

[23] C. Qian, H. Ngan, Y. Liu, and L. M. Ni, "Cardinality estimation for large-scale RFID systems," *IEEE Trans. Parallel Distrib. Syst.*, vol. 22, no. 9, pp. 1441–1454, Sep. 2011.

[24] Y. Zheng and M. Li, "Pet: Probabilistic estimating tree for large-scale RFID estimation," *IEEE Trans. Mobile Comput.*, vol. 11, no. 11, pp. 1763–1774, Nov. 2012.

[25] F. Schoute, "Dynamic frame length aloha," *IEEE Trans. Commun.*, vol. 31, no. 4, pp. 565–568, Apr. 1983.

[26] W. Su, N. V. Alchazidis, and T. T. Ha, "Multiple RFID tags access algorithm," *IEEE Trans. Mobile Comput.*, vol. 9, no. 2, pp. 174–187, Feb. 2010.

[27] M. Buettner and D. Wetherall, "An emprical study of UHF RFID performance," in *Proc. 14th ACM Int. Conf. Mobile Comput. Netw.*, 2008, pp. 223–234.

[28] S. R. Arror and D. D. Deavours, "Evaluation of the state of passive UHF RFD: An experimental approach," *IEEE Syst. J.*, vol. 1, no. 2, pp. 168–176, Dec. 2007.

[29] L. Xie, Q. Li, X. Chen, S. Lu, and D. Chen, "Continuous scanning with mobile reader in RFID systems: An experimental study," in *Proc. ACM 14th ACM Int. Symp. Mobile Ad Hoc Netw. Comput.*, 2013, pp. 11–20.

[30] X. Xu, L. Gu, J. Wang, G. Xing, and S. Cheung, "Read more with less: An adaptive approach to energy-efficient RFID systems," *IEEE J. Sel. Areas Commun.*, vol. 29, no. 8, pp. 1684–1697, Sep. 2011.

[31] Y. Yin, L. Xie, J. Wu, A. V. Vasilakos, and S. Lu, "Focus and shoot: Efficient identification over RFID tags in the specified area," in *Proc. 10th Int. Conf. Mobile Ubiquitous Syst.: Comput., Netw. Services*, 2014, pp. 344–357.

[32] S. Tang, J. Yuan, X. Li, G. Chen, Y. Liu, and J. Zhao, "RASPberry: A stable reader activation scheduling protocol in multi-reader RFID systems," in *Proc. IEEE 17th Int. Conf. Netw. Protocols*, 2009, pp. 304–313.

[33] L. Yang, J. Han, Y. Qi, C. Wang, T. Gu, and Y. Liu, "Season: Shelving interference and joint identification in large-scale RFID systems," in *Proc. IEEE INFOCOM*, 2011, pp. 3092–3100.

Yafeng Yin received the BE degree in computer science from Nanjing University of Science and Technology, China in 2011. She is currently working toward the PhD degree in the Department of Computer Science and Technology, Nanjing University. Her research interests include RFID systems and smart phones. She is a student member of the IEEE.

Sanglu Lu received the BS, MS, and PhD degrees from Nanjing University, China, in 1992, 1995, and 1997, respectively, in computer science. She is currently a professor in the Department of Computer Science and Technology, Nanjing University. Her research interests include distributed computing and pervasive computing. She is a member of the IEEE.
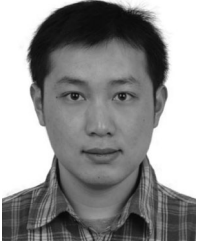
Lei Xie received the BS and PhD degrees from Nanjing University, China, in 2004 and 2010, respectively, in computer science. He is currently an associate professor in the Department of Computer Science and Technology, Nanjing University. His research interests include RFID systems, pervasive and mobile computing, and Internet of Things. He has published more than 40 papers in the *IEEE Transactions on Mobile Computing*, *IEEE Transactions on Parallel and Distributed Systems*, *IEEE Communications Surveys and Tutorials*, ACM MobiHoc, IEEE INFOCOM, IEEE ICNP, IEEE ICC, etc. He is a member of the ACM, IEEE, and a senior member of the CCF.

Jie Wu is the chair and a Laura H. Carnell professor in the Department of Computer and Information Sciences, Temple University. He is also an Intellectual Ventures endowed visiting chair professor in the National Laboratory for Information Science and Technology, Tsinghua University. Prior to joining Temple University, he was a program director in the National Science Foundation and was a distinguished professor in Florida Atlantic University. His current research interests include mobile computing and wireless networks, routing protocols, cloud and green computing, network trust and security, and social network applications. He regularly publishes in scholarly journals, conference proceedings, and books. He serves on several editorial boards, including the *IEEE Transactions on Service Computing* and the *Journal of Parallel and Distributed Computing*. He was a general co-chair/chair for the IEEE MASS 2006, IEEE IPDPS 2008, IEEE ICDCS 2013, and ACM MobiHoc 2014, as well as a program co-chair for the IEEE INFOCOM 2011 and CCF CNCC 2013. He was an IEEE Computer Society distinguished visitor, ACM distinguished speaker, and a chair for the IEEE Technical Committee on Distributed Processing (TCDP). He received the 2011 China Computer Federation (CCF) Overseas Outstanding Achievement Award. He is a CCF distinguished speaker and a fellow of the IEEE.